2020 IEEE International Conference on Robotics and Automation (ICRA)
31 May - 31 August, 2020. Paris, France

A Variable-Fractional Order Admittance Controller for pHRI

Doganay Sirintuna[1*], Yusuf Aydin[1*], Ozan Caldiran[1], Ozan Tokatli[2], Volkan Patoglu[3], and Cagatay Basdogan[1]

***Abstract*— In today's automation driven manufacturing environments, emerging technologies like cobots (collaborative robots) and augmented reality interfaces can help integrating humans into the production workflow to benefit from their adaptability and cognitive skills. In such settings, humans are expected to work with robots side by side and physically interact with them. However, the trade-off between stability and transparency is a core challenge in the presence of physical human robot interaction (pHRI). While stability is of utmost importance for safety, transparency is required for fully exploiting the precision and ability of robots in handling labor intensive tasks. In this work, we propose a new variable admittance controller based on fractional order control to handle this trade-off more effectively. We compared the performance of fractional order variable admittance controller with a classical admittance controller with fixed parameters as a baseline and an integer order variable admittance controller during a realistic drilling task. Our comparisons indicate that the proposed controller led to a more transparent interaction compared to the other controllers without sacrificing the stability. We also demonstrate a use case for an augmented reality (AR) headset which can augment human sensory capabilities for reaching a certain drilling depth otherwise not possible without changing the role of the robot as the decision maker.**

I. INTRODUCTION

Collaborative robots (cobots) are expected to play a vital role in the manufacturing and automation sector in the future. A recent analysis shows that, unlike the initial vision of Industry 4.0, workers will not be completely replaced by fully automated factories; instead, they will work side by side in collaboration with cobots to surpass fully automated systems [1]. Cobots are expected to provide manufacturers with safe, versatile, flexible and easy-to-use tools to support human operators. Moreover, cobots may help to reduce the ergonomic concerns of workers that arise due to excessive physical and cognitive loading [2].

During the last ten years, the number of cobots has increased significantly not only in large manufacturing companies, but also in small and medium size ones due to their relatively lower cost and easier integration into assembly lines [3]. So far, they have been used in applications such as transportation of heavy or bulky objects, assembling parts, precise positioning and orientation of machining tools with respect to a workpiece. (see the review by Ajoudani et al. [4]).

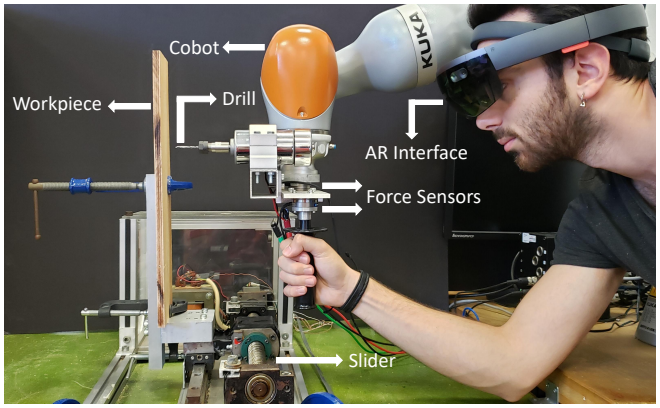

Fig. 1: Experimental Setup.

In all of the above applications, there exists a physical interaction between human and cobot. An important research topic in physical Human-Robot Interaction (pHRI) is ensuring the safety, in particular reducing risk of injuries to the human operator during the collaborative execution of a task. Although the data collected by various sensors can be used to improve human safety, for instance by avoiding collisions or stopping the robot when necessary, a key issue to guarantee safety remains to be the design of a stable interaction controller. This is highly challenging since the controller design should take into account the human and environment impedance, which are typically not known a priori. Moreover, changing requirements of complex collaborative tasks may result in variations of those impedance, which calls for the parameters of interaction controller to be adapted in real-time accordingly, for more effective collaboration and better task performance.

For example, assume a worker in a manufacturing environment needs to drill a hole on a certain location of a curved workpiece with a certain angle. Typically, performing this operation using a standard drill press requires multiple steps and the use of some auxiliary pieces such as a center punch to mark the hole location, fixtures to hold the curved workpiece in place with respect to the drill axis, and jigs to guide the drill bit towards the workpiece. Now, imagine that the worker performs the same operation in collaboration with a robot using a portable drill rigidly attached to its end effector. Here, the worker initially needs to bring the end effector of robot (and hence the drill) close to the proper configuration on the curved workpiece with minimal resistance from the robot

The Scientific and Technological Research Council of Turkey (TUBITAK) supported this work under contract EEEAG-117E645.

*The first two authors contributed equally to this work.

[1]Doganay Sirintuna, Yusuf Aydin, Ozan Caldiran, and Cagatay Basdogan are with College of Engineering, Koc University, 34450, Istanbul, Turkey

[2]Ozan Tokatli is with RACE UKAEA, Abingdon, OX14 3DB, UK

[3]Volkan Patoglu is with Faculty of Engineering and Natural Sciences, Sabanci University, Istanbul, 34956, Turkey

#Corresponding author: cbasdogan@ku.edu.tr

(transparency), then the robot can provide haptic guidance to the worker and lock to the drill orientation, and finally the worker applies sufficient pressure to advance the drill bit into the workpiece while the controller maintains the stability of interaction for safe operation. Here, worker's adaptability in decision-making is augmented with the robot's ability to carry loads and provide support.

As obvious from this sample pHRI scenario, the contradicting nature of transparency (minimum resistance to human operator initially) and robust stability (maximum safety for human operator during the drilling) makes the design of interaction controller challenging. In this paper, we propose a fractional order adaptive admittance controller for pHRI systems to improve performance while ensuring safety during a collaborative task, especially involving contacts with the environment. The proposed approach extends our earlier work on fractional order admittance controller (FOAC) [5] by adapting the admittance parameters of the robot in real-time during the task to balance the trade-off between the stability and the transparency of the coupled system. Compared to an integer order adaptive admittance controller, a fractional order controller enables the adjustment of the order of fractional derivative, which brings an additional flexibility in controlling the dynamics of interactions between human operator and robot. In particular, adapting the order of fractional derivative enables the admittance parameters to become frequency-dependent, which can be tuned to handle changes in interaction dynamics, due to fluctuations in human and environment impedance.

In order to investigate the effectiveness of the proposed approach, we conduct a pHRI experiment in a laboratory environment. This experiment imitates the task that a worker typically performs with a hand-held power tool in an industrial setting. In this experiment, the participants use a power drill rigidly attached to the end effector of a KUKA LBR iiwa 7 R800 robot to drill at different locations holes on a flat vertical wooden workpiece (see Fig. 1). Here, the role of the robot is to show minimal resistance (transparency) to human while moving in free space, fix the drill angle (i.e., keep the power drill along the direction of drill angle all the time), and reduce the contact instabilities during drilling. We show that, in comparison to the integer order adaptive admittance controller, the proposed fractional order adaptive admittance controller reduces the human effort, task completion time, and amplitude of contact forces, when both controllers are designed to be robust against the oscillations induced by the drill. Moreover, an AR interface (HoloLens, Microsoft Inc.) is used to inform the participant about the drill depth and when to stop drilling.

A. Related Work

A classical interaction controller with fixed parameters may not be flexible enough to accommodate changes in dynamical behavior of human, and task requirements, which may frequently occur during the execution of a collaborative task. On the other hand, adaptive interaction controllers are shown to be promising alternatives. For the success of such controllers in pHRI, their design must pay utmost attention on the coupled stability. Coupled stability implies the safety of human operator by guaranteeing the safe operation of the robot; therefore, it is an indispensable aspect for any pHRI application. However, due to the complexity introduced by the presence of human operator and possible contact interactions with uncertain environments, stability characteristics of pHRI systems cannot be analyzed easily.

It has been reported in the literature that the stiffness components of both the human arm and the environment models are particularly important as they have a direct effect on the coupled stability of the interaction [5]–[7]. Under the light of this information, Gallagher et al. [8] estimated the human arm stiffness using EMG sensors to adjust the gains of an impedance controller on-the-fly, while ensuring stability of the coupled system. Similarly, Lamy et al. [9] measured the grasping force applied by human to estimate the arm stiffness to adapt the robot controller accordingly. This method requires the design of a gain scheduler and physical handles equipped with pressure sensors for implementation.

In the absence of human and environment models, the coupled stability of pHRI systems can be investigated using the passivity framework [10], [11]. Passivity can guarantee the stability of the closed-loop system for a broad range of human/environment models; however, the resulting controller performs conservatively [11], [12], leading to a less transparent system.

Satisfying passivity throughout the interaction ensures that energy is not generated, so that stability can be guaranteed for a large range of human/environment impedance. However, non-passive (i.e. active) systems are not necessarily unstable when coupled to an environment [13], [14]. For this reason, instead of maintaining passivity throughout the interaction, researchers have developed alternative online methods by analysing the signals in frequency domain. For instance, Ryu et al. [15] proposed haptic stability observer (HSO) which detects an instability by analyzing first hand measures such as position and force, directly. When HSO detects instability, admittance damping is increased to reassure stability. Later, oscillations in force applied to the robot during a pHRI task were detected using an FFT algorithm and an adaptive admittance controller was proposed to reduce these oscillations [16]. In this regard, Dimeas and Aspragathos proposed an instability index based on the frequency analysis of interaction force. Additionally, they have experimentally shown that increasing admittance mass as well as damping contributes to the stability of the system, when instability is detected [7]. Recently, Ferraguti et al. proposed an improved heuristic method for detecting the emergence of instability and a passivity-preserving inertia adaptation strategy with the use of energy tanks concept [17].

To relax the conservativeness of the frequency domain passivity framework, Hannaford and Ryu [18], proposed time-domain passivity approach which promises stable human-robot interactions, even in the absence of human and environment models. However, this method requires continual estimation of the exchanged energy between the robot and

human and/or environment through sensor measurements, which may prove challenging due to sampling, noise, and quantization effects. Furthermore, abrupt engagement of this controller may disturb the quality of interaction.

B. Contributions

Earlier studies in pHRI have relied on increasing the damping of the controller to increase the stability robustness of a system through energy dissipation. Some alternative approaches adapt the mass and/or the ratio between mass and damping of the controller [7], [15]–[17]. Making such alterations in the controller parameters are shown to be promising and result in better responses than an LTI interaction controller with fixed parameters.

We have proposed a fractional order admittance controller (FOAC) for pHRI systems in [5] and [19]. This control scheme relies on the fractional order calculus, which allows the use of integrators/differentiators of arbitrary orders. We have demonstrated the advantages of FOAC over the classical integer order admittance controllers (IOAC). Specifically, the order of integration enables more effective control of frequency-dependent response of admittance parameters and brings more flexibility to better adjust the trade-off between stability and transparency. These advantages of FOAC make it well-suited for pHRI applications that involve contact interactions. In this study, we further exploit the advantage of FOAC and propose a variable FOAC which is based on the adaptation of the order of the integration. We compare the performance of proposed controller with a classical admittance controller with fixed parameters as a baseline and an integer order variable admittance controller during a realistic drilling task. Besides, we also demonstrate a potential use of an augmented reality interface for the same task, which helps to inform the user about the drill depth and when to stop drilling.

II. Approach

In a typical pHRI setting, an operator and a robot physically interacts with each other and/or their environment. The drilling scenario introduced in the Section I (see Fig. 1) presents an example of such a pHRI setting. For the implementation of this scenario, we utilized the admittance control architecture reported in our earlier study [5] (see Fig. 2). According to this architecture, the operator grasps the power drill connected to the end effector of robot with a desired velocity, v_{des}. To achieve this velocity, she/he exerts a force F_h to the handle. The resultant force due to the interaction of the human, robot, and the environment is acquired by a force sensor with some filter dynamics $H(s)$. The interaction force F_{int} is then inputted to the admittance controller $Y(s)$ of robot to generate a reference velocity profile v_{ref}.

Admittance controllers are designed based on the mechanical admittance of mass-spring-damper systems, resulting in an IOAC. FOAC generalizes these controllers by utilizing fractional order integrators. The FOAC used in this study

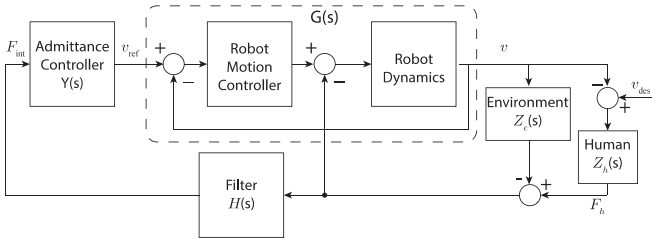

Fig. 2: Control Architecture.

has the following form:

$$Y(s) = \frac{1}{Z_{\text{FOAC}}} = \frac{1}{m_F s^{\alpha} + b_F} \tag{1}$$

where α corresponds to the (fractional) order of the integrator, while m_F and b_F are the admittance controller parameters. In this general form, units of m_F and b_F are $[\mathrm{kg\,s}^{\alpha-1}]$ and $[\mathrm{N\,s\,m}^{-1}]$, respectively. Implementation details of a standard FOAC in real-time can be found in [5].

A. Variable FOAC

In pHRI literature, there are various online methods to estimate the need for increasing stability robustness. Once such a need is detected, parameters of an IOAC are altered on-the-fly accordingly. A similar approach can be adapted to FOAC utilizing the extra degree of freedom that the fractional integration order α introduces.

In this study, we focus our attention on investigating the adaptation of α on task performance. Along these lines, we assume that the monitoring of the stability of interaction is performed by an index/estimator, as proposed in some earlier studies [7], [15]. If an estimator and a controller are used in tandem, then the performance observed in the experiments would also depend on the performance of the estimator, which would be more difficult to evaluate. Therefore, to decouple these effects, we implement a simple adaptation rule for the proposed variable FOAC based on the tool position under the assumption that the requirements of the task are known a priori.

Initially, our task requires a high backdrivability of the robot allowing the user to bring the power drill close to the target location with minimal resistance (transparency) in order to reduce the overall task duration and human effort. Hence, α is chosen as 1 at the start of the interaction. On the other hand, increasing stability robustness for safety is critical during the contact and penetration phases of the task to avoid any injuries. As lower values of α is known to provide higher stability robustness [5], we vary α as a linear function of the distance between drill tip and surface of the workpiece in a way that the lowest α is reached at the contact. In summary, we use the following adaptation strategy:

$$\alpha(d) = \begin{cases} 1 & d \geq d_0 \\ \alpha_c + \frac{d}{d_0}(1-\alpha_c) & d_0 > d \geq 0 \\ \alpha_c & 0 > d \end{cases} \tag{2}$$

where α_c is the integration order of the controller at the contact, and d and d_0 are the instantaneous and initial distances between the drill tip and the workpiece, respectively.

III. Experimental Evaluation

To verify the hypothesized advantages of our adaptive approach, we compare the performance of the proposed variable FOAC (v-FOAC) to a standard IOAC with fixed admittance parameters (f-IOAC) and a variable IOAC (v-IOAC) during a drilling task.

A. Controller Parameters

All controllers were designed by prioritizing the stability of interactions such that the drilling task could be performed safely; we selected a conservative set of effective admittance parameters for all controllers at the contact location ($m_I = 30\,\mathrm{kg}$, $b_I = 2250\,\mathrm{N\,s/m}$). We used these parameters as the admittance mass and damping for v-IOAC at the contact location (see the red curves at normalized distance $d/d_0 = 0$ in Fig. 3) and for f-IOAC during the entire interaction (see the green curves in Fig. 3). On the other hand, for v-FOAC when $\alpha \in (0, 1)$, the effective damping and mass of the system becomes frequency dependent and α is not known a priori. The relations between the admittance mass and damping of IOAC and FOAC can be shown to be

$$\begin{aligned} m_I &= m_F \omega_0^{\alpha-1} \sin\left(\frac{\pi\alpha}{2}\right), \\ b_I &= b_F + m_F \omega_0^{\alpha} \cos\left(\frac{\pi\alpha}{2}\right), \end{aligned} \tag{3}$$

respectively, where ω is the frequency [5], [20], [21].

The admittance matching approach used in [5] utilizes these relations to find an IOAC that matches the admittance of a given FOAC for a frequency of interest ω_0, e.g., the operating frequency of the drill $\omega_0 = 34\,\mathrm{Hz}$. To perform the reverse matching, i.e., find an FOAC that matches a given IOAC, requires additional criterion as three admittance parameters of FOAC have to be estimated from the given two effective admittance parameters using Eq. (3). In our particular case, the goal of maximizing b_I at the contact location can serve as the required criterion:

$$\underset{\alpha}{\operatorname{argmax}}\, b_I = \alpha_{\max} = \frac{2}{\pi} \arctan\left(\frac{2 \ln \omega_0}{\pi}\right). \tag{4}$$

By selecting $\alpha_c > \alpha_{\max}$, one can achieve a monotonically increasing effective damping as the tool tip gets closer to the contact point. To account for the uncertainties related to the operating frequency of the drill, we chose $\alpha_c = 0.85$, a value larger than the calculated $\alpha_{\max}$. Consequently, the remaining parameters of v-FOAC can be calculated as

$$\begin{aligned} m_F &= \frac{m_I\, \omega_0^{1-\alpha_c}}{\sin\left(\frac{\pi\alpha_c}{2}\right)}, \\ b_F &= b_I - \frac{m_I\, \omega_0}{\tan\left(\frac{\pi\alpha_c}{2}\right)}. \end{aligned} \tag{5}$$

Choosing m_F and b_F based on the above approach leads to the most transparent design for v-FOAC while matching the admittance of the conservative f-IOAC at $\omega_0 = 34\,\mathrm{Hz}$. Consequently, the other v-FOAC parameters were determined as $m_F = 69\,\mathrm{kg\,s^{\alpha-1}}$ and $b_F = 711\,\mathrm{N\,s/m}$, respectively.

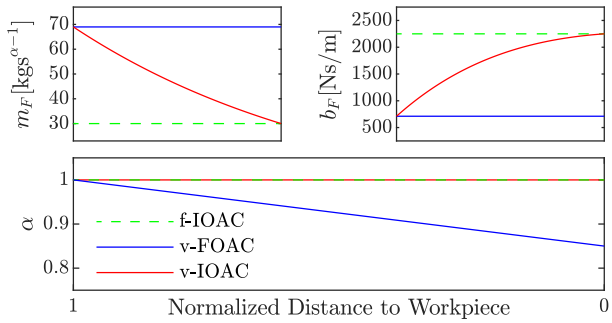

Fig. 3: Controller parameters as functions of normalized distance.

Note that at the beginning of this section, we have only introduced v-IOAC parameters at the contact location only. For a fair comparison of with v-FOAC, we used the same admittance matching approach elsewhere, i.e., v-FOAC and v-IOAC had the same effective admittance along the whole interaction trajectory. Parameters of all controllers are illustrated Fig. 3 as functions of distance of the drill tip to the workpiece.

B. Experimental Setup

The major components of our experimental setup were a power drill, two force sensors (Mini40, ATI Inc.), and a handle attached to the end effector of a LBR iiwa 7 R800 robot (KUKA Inc.) as shown in Fig. 1. One of the force sensors was used to measure the interaction force between the drill bit and the workpiece, while the other one measured the force applied by the user alone. The force data from both sensors was acquired simultaneously at $10\,\mathrm{kHz}$ using a DAQ card (PCI-6225, National Instruments Inc.), though the control loop given in Fig. 2 was updated at $500\,\mathrm{Hz}$. In order to reach to this high update rate, we utilized the Fast Robot Interface (FRI) library of the robot, but implemented the admittance controller by ourselves in C/C++ using the "Joint Position Controller" function of the library and taking advantage of the forward and inverse kinematics reported in [22]. The workpiece was a flat wooden block with dimensions of $400 \times 110 \times 10\,\mathrm{mm}$, which was placed on a moving stage at a distance of $d = 95\,\mathrm{mm}$ from the tip of drill bit. Upon completion of the task, the stage was commanded to move the workpiece aligning the next drilling location and the robot movement direction. The AR interface used in this study (HoloLens, Microsoft Inc.) informed the user about the distance of the drill tip to the workpiece (see Fig. 4a), instantaneous drilling depth, and the targeted drill depth of $5\,\mathrm{mm}$ (see Fig. 4b).

C. Participants

The experiment was conducted with 7 participants (1 female, 6 males). The average age of the participants was 24.9 ± 5.3 years. All participants were graduate students and

right-handed. Participants read and signed the consent form approved by Ethical Committee for Human Participants of Koc University before the experiment.

D. Experimental Procedure

Each participant performed a total of 15 trials (3 interaction controllers $\times$ 5 repetitions). The controllers were presented to the participants in a randomized order. In the first three trials, all three controllers were presented once. These trials were regarded as the training trials and not included in the data analysis.

Each trial consists of 1) a driving phase, where the participants gripped the handle with their dominant hand and guided the robot towards the drilling location (see Fig. 4a), and 2) a penetration phase, which starts with the initial contact of the drill bit to the surface of the workpiece and ends when the desired depth is reached. In the penetration phase, the participants were asked to penetrate into the workpiece to drill a hole with a depth of $5\,\mathrm{mm}$; the instantaneous drilling depth was displayed through the visor of AR interface (see Fig. 4b). During the whole task, the robot was programmed to constrain the movements of the participant along the direction perpendicular to the surface of workpiece.

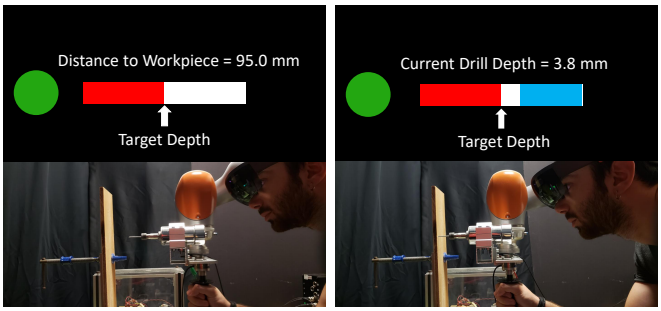

(a) Driving phase (b) Penetration phase

Fig. 4: Visual information displayed to the participants through the AR interface during the execution of drilling task. In the driving phase distance to workpiece was displayed, whereas the current drill depth was displayed during the penetration phase. The green circle in the view indicates that the robot controller is active. The red and white bars represent the cross-section of the workpiece. The red bar shows the part that should not be penetrated, whereas the white bar shows the desired depth that will be drilled. The blue bar grows from right to left as the drill bit penetrates into the workpiece, and shows the current drill depth.

E. Performance Metrics and Statistical Analysis

We defined several performance metrics to compare the task performance of participants under three different controllers

- average interaction force: $F_{\text{int}}^{\text{ave}}$
- average force applied by participant: F_h^{ave}
- average completion time: t^{ave}
- average velocity: v^{ave}
- peak amplitude of oscillations for the end-effector velocity: A_V
- total effort by participant: $E_h^{\text{tot}} = \int_{t_b}^{t} F_h(t)v(t)dt$
- error in drilling depth: ϵ.

We calculated these performance metrics for each phase of our drilling task separately, since the driving and penetration phases have different requirements regarding robust stability and transparency of interaction.

We fitted linear mixed-effects models (LMM) for the statistical analysis to investigate the effect of controller type on performance metrics using the `fitlme` function of MATLAB. We chose to use LMMs as the participants performed multiple trials with the same controllers. In our LMMs, the participants were random effects, and the controller types were the fixed effects. We used `'reference'` dummy variable coding scheme, since the controller type was a categorical variable. In the variable coding, v-FOAC was selected as the reference, i.e., the intercept of the model. Analysis of Variance (ANOVA) was utilized to check the significance level of the parameters with $\alpha = 0.05$, and p values were adjusted using Bonferroni-Holm correction [23], [24].

F. Results

Sample plots of the performance metrics are depicted for one participant in Fig. 5. For each controller type and interaction phase, the mean values of all trials and standard errors of the mean are reported as a function of normalized time.

In Fig. 6, the mean values (average of all participants) of $F_{\text{int}}^{\text{ave}}$, F_h^{ave}, and t^{ave} are plotted for both interaction phases. The mean value of v^{ave} is drawn for the driving phase only since it is an indicator of transparency, while the mean value of A_V is plotted for the penetration phase only as stability is more critical during drilling.

In the driving phase, LMM fitting revealed statistically significant effect of the controller type in general and also significant difference particularly indicating higher transparency of v-FOAC for all metrics, compared to the other two controllers, i.e., smaller completion time, human and interaction forces, and larger velocities. On the other hand, in the penetration phase, there was statistically significant difference only for the force-related metrics $F_{\text{int}}^{\text{ave}}$ and F_h^{ave}. Moreover, the total effort E_h^{tot} was significantly lower in the case of v-FOAC. The related p values were smaller than 0.001 where significant difference was found, and larger than 0.05 where no significant difference was found.

IV. DISCUSSION

We proposed a variable FOAC (v-FOAC) based on the adaptation of integration order α. Effectiveness of the proposed controller was tested in a drilling task by comparing its performance with that of a standard IOAC with fixed parameters (f-IOAC) and an adaptive IOAC (v-IOAC). Since we had to ensure stability of all controllers, we hypothesized that the benefit of v-FOAC would show up in transparency, especially during the driving phase.

Results of our experiment support our hypothesis. Although the participants applied less force to the robot in the case of v-FOAC (Fig. 6c, 6d), they reached higher average velocities (Fig. 6g); hence, completed the task faster

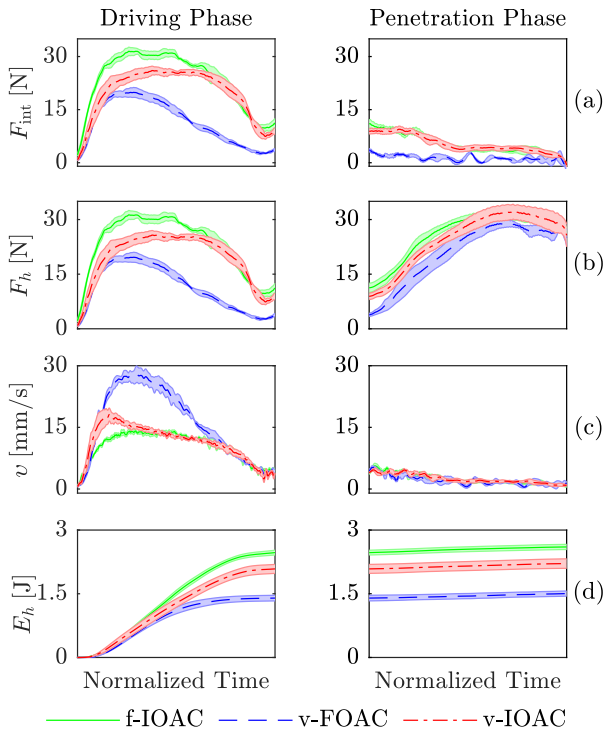

Fig. 5: The variation in performance metrics of one participant as a function of normalized time.

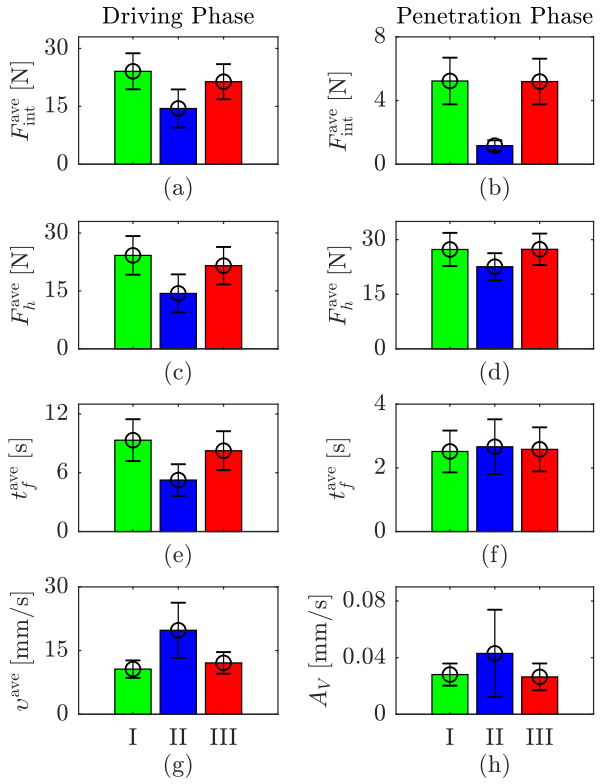

Fig. 6: The means (average of all participants) and standard errors of means for all performance metrics (I: f-IOAC, II: v-FOAC, III: v-IOAC).

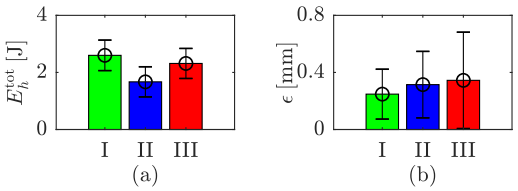

Fig. 7: The means (average of all participants) and standard errors of means for total effort and absolute value of error in drilling depth (I: f-IOAC, II: v-FOAC, III: v-IOAC).

though there were no instructions to do so (Fig. 6e), and put significantly less effort (Fig. 7a). In addition to all these improvements regarding transparency, v-FOAC did not compromise stability or accuracy. Compared to f-IOAC and v-IOAC, the mean value of A_V for v-FOAC was not significantly larger than those of f-IOAC and v-IOAC (Fig. 6h), i.e., v-FOAC provided comparable attenuation for the drilling-related vibrations. Moreover, the accuracy in drilling depth was on par with the other controllers (Fig. 7b).

In summary, as fractional integration order α of the v-FOAC was gradually reduced from 1 to 0.85, the controller displayed a frequency-dependent dissipation. v-FOAC allows for effective damping to increase with frequency, providing further stability robustness at relatively high frequencies, while not significantly interfering with the quality of the interaction at low frequencies where intentional control takes place. However, altering admittance damping under v-IOAC increases the damping at all frequencies, providing good stability robustness in general but compromises from transparency, resulting in a poorer task performance than v-FOAC.

V. CONCLUSION

In this study, we proposed a variable FOAC for pHRI systems and evaluated its presented advantages over v-IOAC and f-IOAC where all the controllers were designed using admittance matching to display similar stability robustness against the undesired effects disturbing the system. The proposed v-FOAC controller outperformed the alternatives in terms of task performance. These results are significant as they provide evidence of the potential of v-FOAC.

Our ongoing work includes determination of adaptation rule for FOAC instead of the simple rule used in this work. We also plan to extend our work to perform high precision drilling operations on curved surfaces, which is more challenging than drilling a flat surface.

ACKNOWLEDGMENT

The Scientific and Technological Research Council of Turkey (TUBITAK) supported this work under contract EEEAG-117E645.

REFERENCES

[1] "Collaborative robot market," https://www.marketsandmarkets.com/Market-Reports/collaborative-robot-market-194541294.html, accessed: 2019-09-10.

[2] A. Cherubini, R. Passama, A. Crosnier, A. Lasnier, and P. Fraisse, "Collaborative manufacturing with physical human–robot interaction," *Robotics and Computer-Integrated Manufacturing*, vol. 40, pp. 1 – 13, 2016.

[3] V. Villani, F. Pini, F. Leali, and C. Secchi, "Survey on human-robot collaboration in industrial settings: Safety, intuitive interfaces and applications," *Mechatronics*, vol. 55, pp. 248 – 266, 2018.

[4] A. Ajoudani, A. M. Zanchettin, S. Ivaldi, A. Albu-Schäffer, K. Kosuge, and O. Khatib, "Progress and prospects of the human–robot collaboration," *Autonomous Robots*, vol. 42, no. 5, pp. 957–975, Jun 2018.

[5] Y. Aydin, O. Tokatli, V. Patoglu, and C. Basdogan, "Stable physical human-robot interaction using fractional order admittance control," *IEEE Transactions on Haptics*, vol. 11, no. 3, pp. 464–475, July 2018.

[6] T. Tsumugiwa, R. Yokogawa, and K. Yoshida, "Stability analysis for impedance control of robot for human-robot cooperative task system," in *IEEE/RSJ International Conference on Intelligent Robots and Systems*, 2004, pp. 3883–3888.

[7] F. Dimeas and N. Aspragathos, "Online stability in human-robot cooperation with admittance control," *IEEE Transactions on Haptics*, vol. 9, no. 2, pp. 267–278, 2016.

[8] W. Gallagher, D. Gao, and J. Ueda, "Improved stability of haptic human–robot interfaces using measurement of human arm stiffness," *Advanced Robotics*, vol. 28, no. 13, pp. 869–882, 2014.

[9] X. Lamy, F. Colledani, F. Geffard, Y. Measson, and G. Morel, "Achieving efficient and stable comanipulation through adaptation to changes in human arm impedance," in *IEEE International Conference on Robotics and Automation*, May 2009, pp. 265–271.

[10] J. E. Colgate and N. Hogan, "Robust control of dynamically interacting systems," *International Journal of Control*, vol. 48, no. 1, pp. 65–88, 1988.

[11] J. E. Colgate and G. G. Schenkel, "Passivity of a class of sampled-data systems: Application to haptic interfaces," *Journal of Robotic Systems*, vol. 14, no. 1, pp. 37–47, 1997.

[12] T. Hulin, A. Albu-Schäffer, and G. Hirzinger, "Passivity and stability boundaries for haptic systems with time delay," *IEEE Transactions on Control Systems Technology*, vol. 22, no. 4, pp. 1297–1309, July 2014.

[13] S. P. Buerger, H. I. Krebs, and N. Hogan, "Characterization and control of a screw-driven robot for neurorehabilitation," in *IEEE International Conference on Control Applications*, 2001, pp. 388–394.

[14] S. P. Buerger and N. Hogan, "Complementary stability and loop shaping for improved human–robot interaction," *IEEE Transactions on Robotics*, vol. 23, no. 2, pp. 232–244, April 2007.

[15] D. Ryu, J. Song, J. Choi, S. Kang, and M. Kim, "Frequency domain stability observer and active damping control for stable haptic interaction," in *IEEE International Conference on Robotics and Automation*, April 2007, pp. 105–110.

[16] V. Okunev, T. Nierhoff, and S. Hirche, "Human-preference-based control design: adaptive robot admittance control for physical human-robot interaction," in *IEEE RO-MAN: The 21st International Symposium on Robot and Human Interactive Communication*, Sept 2012, pp. 443–448.

[17] F. Ferraguti, C. T. Landi, L. Sabattini, M. Bonfè, C. Fantuzzi, and C. Secchi, "A variable admittance control strategy for stable physical human–robot interaction," *The International Journal of Robotics Research*, vol. 38, no. 6, pp. 747–765, 2019.

[18] B. Hannaford and J.-H. Ryu, "Time-domain passivity control of haptic interfaces," *IEEE Transactions on Robotics and Automation*, vol. 18, no. 1, pp. 1–10, Feb 2002.

[19] Y. Aydin, O. Tokatli, V. Patoglu, and C. Basdogan, "Fractional order admittance control for physical human-robot interaction," in *IEEE World Haptics Conference (WHC)*, June 2017, pp. 257–262.

[20] O. Tokatli and V. Patoglu, "Stability of haptic systems with fractional order controllers," in *IEEE/RSJ International Conference on Intelligent Robots and Systems*, Sept 2015, pp. 1172–1177.

[21] O. Tokatli and V. Patoglu, *Using Fractional Order Elements for Haptic Rendering*. Cham: Springer International Publishing, 2018, pp. 373–388.

[22] C. Faria, F. Ferreira, W. Erlhagen, S. Monteiro, and E. Bicho, "Position-based kinematics for 7-dof serial manipulators with global configuration control, joint limit and singularity avoidance," *Mechanism and Machine Theory*, vol. 121, pp. 317 – 334, 2018. [Online]. Available: http://www.sciencedirect.com/science/article/pii/S0094114X17306559

[23] S. Holm, "A simple sequentially rejective multiple test procedure," *Scandinavian Journal of Statistics*, vol. 6, no. 2, pp. 65–70, 1979.

[24] D. Groppe, "Bonferroni-holm correction for multiple comparisons," 2020. [Online]. Available: https://www.mathworks.com/matlabcentral/fileexchange/28303-bonferroni-holm-correction-for-multiple-comparisons (Accessed February 24, 2020).